J Mater Sci (2012) 47:852–859
DOI 10.1007/s10853-011-5863-3

Carbon supported silver (Ag/C) electrocatalysts for alkaline membrane fuel cells

Rajangam Vinodh · Dharmalingam Sangeetha

Received: 21 June 2011 / Accepted: 8 August 2011 / Published online: 24 August 2011

Abstract This study reports on the performance of activated carbon supported silver catalyst (Ag/C) as electrocatalyst in an alkaline membrane fuel cell (AMFC), using alkalized poly (styrene ethylene butylene poly styrene) [APSEBS] as the electrolyte membrane. Carbon supported silver catalyst (Ag/C) with different metal loading was synthesized by means of wet impregnation method. The prepared electrocatalyst was characterized by X-ray diffraction pattern (XRD), thermogravimetric analysis (TGA), UV–Visible diffuse reflectance spectra (DRS-UV) and Raman spectroscopy. Surface morphology analysis of the prepared electrocatalyst using scanning electron microscopy (SEM) revealed the heterogeneous distribution of Ag on carbon support. The performance of the prepared electrocatalyst was evaluated with a home made AMFC using a novel anion exchange membrane (APSEBS). A maximum cell voltage and power density of 0.69 V and 109 mW/cm^2, respectively, was achieved at 60 °C for the home made 10 wt% (Ag/C) cathode catalyst and anion exchange membrane. Further, the prepared electrocatalyst was subjected to cyclic voltammetry studies to evaluate the methanol oxidation for Direct methanol alkaline fuel cell (DMAFC) applications.

Introduction

Today, fuel cells are widely considered to be an efficient and non-polluting power source, offering much higher energy densities and energy efficiencies as compared to any other current energy storage devices. Fuel cells are therefore considered to be promising energy devices for the transport, mobile, and stationary sectors [1–4]. Fuel cells are electrochemical energy conversion devices that convert chemical energy directly into electrical energy. Furthermore, the power generated by a fuel cell depends largely upon the catalytic electrodes and materials used [1–4].

In the last few decades, different types of fuel cell have been developed depending on the type of electrolytes used [5], such as Proton exchange membrane fuel cell (PEMFC), Direct methanol fuel cell (DMFC), Phosphoric acid fuel cell (PAFC), Molten carbonate fuel cell (MCFC), Solid oxide fuel cell (SOFC), and Alkaline fuel cell (AFC). Among these, PEMFC has been extensively explored for wide range of applications in the past two decades [6] due to its quick startup and high power density which are particularly suitable for transportation, portable devices, and stationary power applications [5–7]. Acidic polymer electrolytes (e.g., Nafion) are commonly used in PEMFCs. However, unsolved problems remain in PEMFCs including the high cost of membranes, complex water management and sluggish reaction kinetics [8]. To overcome PEMFC limitations, anion exchange membrane (AEM) has been developed for Alkaline Membrane Fuel Cell (AMFC) applications. AMFC can potentially address many of the drawbacks of PEMFCs including more facile electrokinetics, lower fuel cross over, reduced CO poisoning and use of non-precious metal catalysts [9].

The main objective in fuel cell technologies is to develop low cost, high performance and durable materials (membrane and catalyst). At present, fuel cell systems are too expensive and not durable [4]. However, there are several ways to reduce the cost and increase the performance of a fuel cell such as [10, 11] (i) decreasing the catalyst loading in the fuel cell electrodes, (ii) decreasing

R. Vinodh · D. Sangeetha (✉)
Department of Chemistry, Anna University, Chennai 600025, Tamil Nadu, India
e-mail: sangeetha@annauniv.edu

the size of the catalyst nanoparticles, (iii) developing metallic alloy electrocatalysts, (iv) developing Pt-free electrocatalysts, (v) using novel fabrication methods to synthesize catalysts and produce better catalyst dispersion on the fuel cell electrodes, (vi) developing better fuel cell electrode fabrication methods which enable effective catalyst dispersion and utilization, and (vii) using new techniques to increase the mass-transport at the fuel cell electrode surface.

The alkaline membrane fuel cell technology slightly differs from the other fuel cell types, because of the two key components, one is anion exchange membrane and the second one is Pt-free catalyst. In this article, we chose alkalized poly (styrene ethylene butylene poly styrene) [APSEBS] [12], carbon supported platinum (Pt/C) (also called as Vulcan XC-72) and activated carbon supported silver (Ag/C) as an anion exchange membrane, anode and cathode materials, respectively, to fabricate Membrane electrode assembly (MEA).

Noble metals such as Pt, Pd, Ru, and Au supported over carbon materials have been reported to be efficient catalysts for both the PEMFC and DMFC applications. However, the cost and methanol cross-over factors hinder the development of such products into the market. To overcome these factors, researchers look forward to non-noble metal catalysts like Ag, Ni, and Co, etc. The recent developments in fuel cells have emphasized the use of silver (Ag) as a principal and necessary component to fabricate MEA as a cathode material. Silver is classified as a precious metal. Ag is a soft, white metal with a shiny surface. It is the most ductile and malleable metal.

Supported-metal catalysts are widely used in the energy-related and fine-chemical industries. It is well-known that the properties of the supports have great influence on the catalytic performance [13]. In addition, compared with other supports, carbon materials have considerable advantages, such as (1) high specific surface area up to 3000 m^2/g, (2) high stability in acidic and basic media [14], (3) easy modification of textural properties and functional groups, and (4) easy recovery of supported metals by burning off the catalyst. Moreover, the varieties of available forms (e.g., graphite, carbon black (CB), activated carbon (AC), activated carbon fibers (ACF), carbon nanotubes (CNTs), and carbon molecular sieves (CMS)) make carbon materials very attractive as catalysts or supports for metal catalysts [15, 16]. Thus, a resurgence of interest has occurred to synthesize Ag catalyst using activated carbon support.

To the authors' knowledge, however, the catalytic performance of Ag/C catalysts as a cathode material and alkalized poly (styrene ethylene butylene poly styrene) as a polymer electrolyte membrane toward solid alkaline membrane fuel cell and methanol oxidation has not been reported. In this study, Ag/C electrocatalysts containing different amounts of Ag have been prepared and characterized by XRD, TGA, SEM, DRS-UV, and Raman spectroscopy. Finally, the synthesized Ag/C catalysts activities toward AMFC performance and methanol oxidation in alkaline media have been evaluated.

Materials

Silver nitrate ($AgNO_3$, 25 g) and activated carbon were purchased from E-Merck. Both were of analog grades with 99% purity and were used as received without further purification. Vulcan XC-72 (20% of Platinum in carbon support) was purchased from Arora-Mathey Pvt. Ltd. PTFE binder, platinum and IPA was purchased from Sigma-Aldrich (USA). Carbon cloth was obtained from Cabot carbon Inc.

Experimental

Preparation of Ag/C catalyst

Impregnation method

In the impregnation technique, the carbon support is in contact with a solution containing the salt of a metal catalyst. Impregnation occurs by capillary action. Drawing the salt solution into the porous structure of the support and subsequent evaporation of the solution results in precipitation of metal salt in the pores of the support. In the case of supported metal catalysts, dispersion and distribution of the active phase are largely determined by the impregnation step. A limitation of the impregnation technique is that the surface area of metal particles (m^2/g) decreases as the metal loading increases. This occurs when the metal salt concentrates in a fixed number of pores; as the salt concentration increases, a larger mass of salt is precipitated in each pore (pore-concentration mechanism) and as a result larger metal particles are obtained when the metal salt is reduced. A brief experimental procedure involved in the synthesis of Ag/C catalyst is as follows. The metal precursor, $AgNO_3$ with different weight ratios (2, 4, 6, 8, and 10 wt%) was first dissolved completely in deionized water. Activated carbon powders were then suspended in the resulting solution under vigorous stirring. After a homogeneous suspension was formed, the resultant precipitate was collected by filtration, washed several times with water and dried at 100 °C in an oven and calcined in air at 350 °C for 4 h. Finally, reduction was carried out using H_2 as the reducing agent with flow rate of 700 mL/min at 250 °C for 2 h [17].

Techniques

X-ray diffraction pattern

X-ray diffraction (XRD) is a versatile, non-destructive technique that reveals detailed information about the chemical composition and crystallographic structure of natural and manufactured materials. The X-ray diffraction pattern of a pure substance is, therefore, like a fingerprint of the substance. The powder diffraction method is thus ideally suited for characterization and identification of polycrystalline phases.From the XRD results we can predict the particle size of the crystals by using the Debye–Scherrer formula [18],

$$t = \frac{K\lambda}{\beta\cos\theta}(\text{nm}) \quad (1)$$

where, t is the averaged dimension of crystallites in nanometer; K is the Scherrer constant, arbitrary value that falls in the range 0.87–1.0 (it is usually assumed to be 0.9) and β is the integral breadth of a reflection (in radians) located at 2θ.

UV–Visible diffuse reflectance spectra

UV–Vis DRS were recorded on a T 90+ (PG Instruments) UV–Visible spectrometer, in the wavelength range of 190–800 nm with a scanning speed of 100 nm/min.

Raman spectroscopy

The Raman spectra were recorded based on Raman R3000 System and by using a 50× working-length objective (8 mm). The exciting wavelength was 532 nm with radiation from a He–Ar laser with a power of 0–90 mW at the surface of the sample and a spot of ca. 3 μm on the sample surface. 2 and 10 wt% Ag/C of prepared samples were placed in a specially designed quartz in situ Raman sample cell. The surface of the sample was extensively cleaned at 500 °C under a flow of purified air for about 30 min.

Scanning electron microscopy

A scanning electron microscopy was used to investigate the surface morphology and distribution of Ag on the carbon surface. SEM micrographs of 2 and 10 wt% of Ag/C were obtained with the help of HITACHI S-3400 with associated energy dispersive X-ray analyzer. Ag/C catalysts were dried and then coated with gold to achieve SEM images.

Thermogravimetric analysis

This is the technique in which the change in weight of a substance with temperature over a period of time is followed. Thermal stability and decomposition temperature of the prepared catalysts (Ag/C) can be assessed easily using this technique. The TGA thermal analysis was carried out using TGA model Q50 V20.6 build 31 systems. The measurements were conducted by heating from room temperature to 800 °C at a heating rate of 10 °C/min under nitrogen atmosphere.

Hydroxyl conducting membrane

The membrane used in this study was alkalized poly (styrene ethylene butylene poly styrene) obtained from poly (styrene ethylene butylene poly styrene) by a three step method—Chloromethylation, Quaternization, and followed by Alkalization. The synthesis and characterization procedure of APSEBS was already reported in our previous papers [12, 19]. The main properties of the membrane are tabulated in the Table 1.

Preparation of membrane electrode assembly [20]

The MEA is one of the most important component impacting the overall performance of AMFC. The MEA structure is composed of an electrolyte membrane coated by a catalyst on both the anode and cathode sides and sandwiched by a gas diffusion layer.

Gas diffusion layer preparation

The purpose of the gas diffusion layers is to form an electronic and thermal contact between the electrodes and the flow field plates, and to provide transport paths for the reactant gases and water. The criteria of a gas diffusion layer material are high electrical and thermal conductivity, high porosity, an optimal combination of hydrophobic and hydrophilic properties, good chemical and mechanical durability, and low cost; the most commonly used material is carbon cloth.

The procedure for the preparation of the diffusion slurry ink included mixing 70 wt% Vulcan XC—72 carbon, 30 wt% PTFE binder solutions, and a suitable amount of double distilled water and isopropyl alcohol. The resulting black mixture was first ultra sonicated for 1 h. The black ink was then coated onto the carbon cloth, dried in a

Table 1 Lab prepared APSEBS membrane specifications

Properties of anion exchange membrane	
Water absorption	4.04%
Anion exchange capacity	0.958 meq/g.
Ionic conductivity	1.51×10^{-2} S/cm
Thermal stability	<400 °C
Glass transition temperature	86 °C

vacuum oven at 100 °C for 2 h and then kept in muffle furnace at 350 °C for 6 h.

Preparation of the anode and cathode electrodes

After the preparation of the diffusion layer, catalyst slurry ink was prepared with the help of carbon supported platinum black and silver catalyst with loading of 0.375 and 0.5 mg/cm^2, respectively, for the anode and cathode. Then a suitable amount of double distilled water and isopropyl alcohol were mixed well using ultra sonicator. After the ultra sonication, the black catalyst slurry was coated on to the respective diffusion layers. The prepared anode and cathode were dried in a vacuum oven at 100 °C for 2 h and then in muffle furnace at 350 °C for 6 h. For AMFCs, the platinum loading of anode was thrice greater than cathode due to the water molecules produced at the anode side. While, in polymer electrolyte membrane fuel cells (PEMFCs), the process of platinum loading is reverse.

Fabrication of MEA

The hydroxyl conducting membrane was sandwiched between the prepared anode and cathode electrodes and hot pressed at 80 °C with 1.5 ton pressure for 2 min.

The schematic representation of MEA is shown in Fig. 1.

Fuel cell tests configuration

The fuel cell tests were carried out using in-house fuel cell test station. Membrane electrode assemblies (MEAs), 25 cm^2 were produced by hot pressing. The MEA was secured between two graphite plates which had machined triple serpentine flow channels (1 mm channel width, 1 mm channel height, and 1.5 mm rib width) and gold coated aluminum current collector plates. The fixture was sealed at a constant torque of 5.5 N m, using bolts and a torque wrench. Fuel cell measurements were carried out at 60 °C with H_2 and O_2 gases.

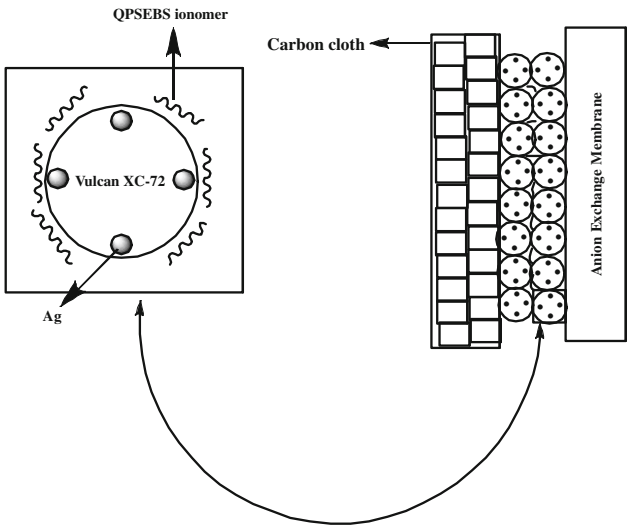

Fig. 1 Schematic representation of cathode side (carbon cloth/Ag-C/AEM) in the membrane electrode assembly using Ag/C as a catalyst

Table 2 Experimental conditions for MEA and AMFC operation

AMFC	Anode	Cathode
Catalyst	Pt/C	Ag/C
Catalyst loading (mg/cm^2)	0.375	0.5
Active area (cm^2)	5	5
Fuel/oxidant	H_2	O_2
Cell temperature (°C)	60	60

The brief experimental condition for MEA and AMFC operation were summarized in Table 2.

Methanol oxidation

The electrochemical activity of 10 wt% Ag/C was measured for the electro-oxidation of methanol. As a typical process, 1 mg of electrocatalyst sample was ultrasonically mixed in 200 μL of water solution to form a homogeneous ink followed by dropping 4 μL of the electrocatalyst ink onto the surface of a glassy carbon electrode (GCE) with an area of 0.0707 cm^2. Then, 5 μL of APSEBS ionomer was added to fix the electrocatalyst on the GCE surface. Pt foil and saturated calomel electrode (SCE) was used as the counter and reference electrodes, respectively. All potentials given in this study were with respect to SCE reference electrode. The potential window was fixed from −0.2 to 0.8 V with the scan rate of 50 mVs^{-1}.

Results and discussion

XRD

The as prepared Ag/C catalysts were characterized by XRD the spectra of which are shown in Fig. 2. XRD is a bulk analysis that reveals the crystal structure, lattice constant, and crystal orientation of supported catalysts. In the figure, the broad peak at $2\theta = 25.9°$ is associated with (002) plane of the graphite-like structure of the activated carbon, and the diffraction peaks at $2\theta = 38°$, 44°, 64°, and 77° can be attributed to the (111), (200), (220), and (311) crystalline planes, respectively, of the face centered cubic (fcc) structure of Ag [21] (JCPDS 04-0783). A diffraction peak of graphite at $2\theta = 25.9°$ was found to slightly decrease with increase in the percentage of the metal loading. At one

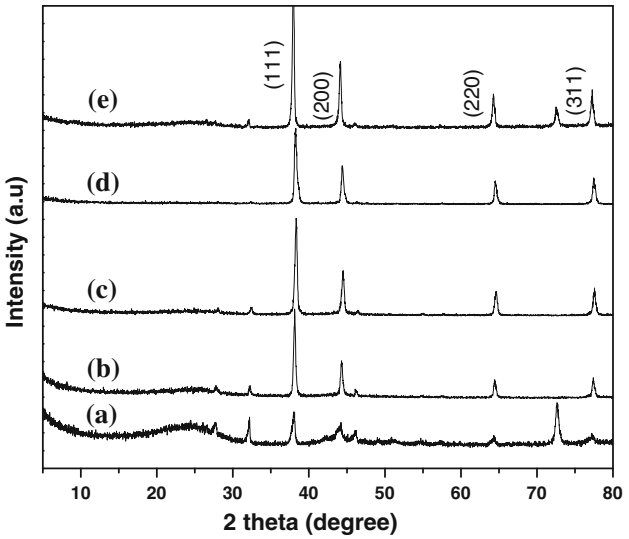

Fig. 2 XRD patterns of (*a*) 2 wt%, (*b*) 4 wt%, (*c*) 6 wt%, (*d*) 8 wt%, and (*e*) 10 wt% as synthesized Ag/C catalyst

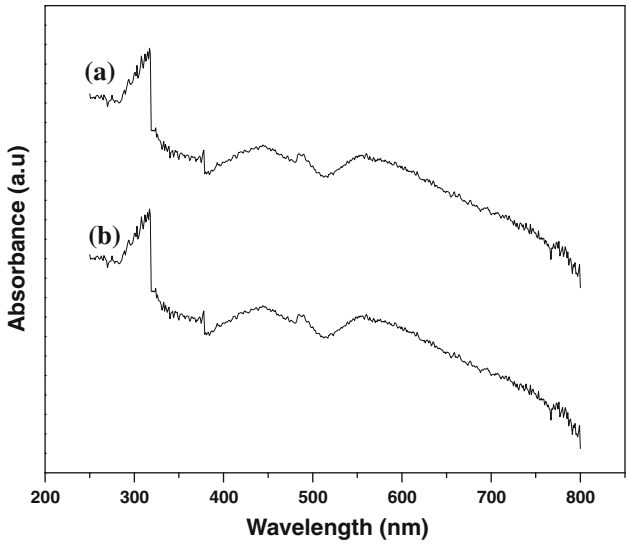

Fig. 3 UV–Vis diffuse reflectance spectra of as-prepared Ag/C catalysts 2 wt% (*a*) and 10 wt% (*b*)

stage, in particular 10 wt% of Ag, the peak completely vanished. This was a result of the strong interaction between the carbon support and the incorporated silver particles indicating that the metal particles were well-distributed within the activated carbon matrix. The average size of the metal particles was calculated based on the (111) facets of diffraction peaks according to Scherrer's equation [18]. The average size of Ag particles was 5.36 nm in 2 wt%, 5.65 nm in 4 wt%, 6.24 nm in 6 wt%, 7.62 nm in 8 wt%, and 10.71 nm in 10 wt%. The analysis revealed that the size of the prepared Ag particles were in nanometer range varying from 5 to 11 nm. The advantage of the nanometer sized particles is their high surface area which would drastically reduce the amount of catalyst required and thus becoming cost effective.

DRS-UV

The UV–Visible diffuse reflectance spectra of the as prepared 2 and 10 wt% Ag/C catalysts are shown in Fig. 3. Four overlapped bands centered at about 266, 316, 440, and 560 nm can be identified in the two samples. There were absorption bands between 400 and 750 nm. They were assigned to surface plasma resonance band of silver nanoparticles. The absorption bands at 266 and 316 nm correspond to the absorption of Ag_4^+ and Ag_5 nanoparticles, respectively, as reported by Aenglein et al. [22]. In addition as suggested by Sato et al. [23], the bands in the range of 240–270 and 275–320 nm correspond to the absorption of $Ag_n^{\delta+}$ and Ag_m nanoparticles, respectively. The difference absorption bands are due to different in size and shape of Ag nanoparticles. There is an absorption band close to 316 nm, it may be assigned to Ag are very small

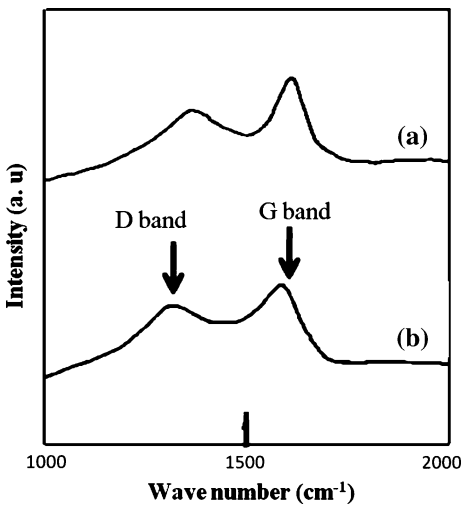

Fig. 4 Raman spectra of Ag/C (*a*) 2 wt% and (*b*) 10 wt% Ag/C

dimensions. In other words, the absorption bands detected over the catalysts described in the study at about 266 and 316 nm can be attributed to small size cationic particles and silver particles, respectively [24].

Raman spectroscopy

The Raman spectra were also used to study the surface structure of prepared Ag/C catalysts and the results were shown in Fig. 4. Both the samples (2 and 10 wt% Ag/C) exhibited two distinct bands appearing at around 1350 (D-band) and 1575 (G-band) cm^{-1}. The D-band and G-band reflect the structure of sp^3 and sp^2 hybridized carbon atom, indicating disordered graphite and the order

state on the Ag/C surfaces, respectively [25]. Therefore, the degree of the graphitization of Ag/C can be quantified by the intensity of ratio of the D to G bands. The peak intensity ratios (I_D/I_G) are 0.51 and 0.46 for the 2 and 10 wt% of Ag/C, respectively. High I_D/I_G ratio indicates that the sample contains high quantities of amorphous carbon impurities. However, in our case, the I_D/I_G ratios obtained were of low value implying that the prepared catalysts possessed good electrical conductivity and corrosion resistance. Hence, these materials could be potentially employed as a cathode material for alkaline membrane fuel cell applications [26, 27].

SEM

Electron microscopic examination is useful in evaluating the special distribution and size of the Ag crystallites in the supported catalyst, since the densities of Ag and activated carbon are significantly different from each other.

Figure 5 illustrates SEM images of 2 wt% (a, b, and c) and 10 wt% (d, e, and f) of activated carbon supported Ag catalysts with different magnifications. The crystal-grown state and surface morphology of silver on the activated carbon surface were observed by scanning electron microscopy. The fine particles and aggregated metallic Ag particles were observed on the surfaces of some activated carbon as indicated in Fig. 5. As is evident from the figure, the aggregations of metallic Ag particles were found to increase with increasing amount of Ag content. From these results, one can easily observe the heterogeneously distributed metallic Ag particles on the carbon surface. The average size of the Ag particle distributed on the carbon surface was 8–10 nm, which is in good agreement with XRD results.

TGA

Figure 6 shows the thermogravimetric graphs for the as synthesized Ag/C catalysts with different weight percentage of metal loading. From this figure, it was found that, in all five thermograms weight loss occurred in two stages. While the first weight loss, i.e., around 90 °C corresponded to the removal of moisture present in the prepared catalyst, the second weight loss at around 580 °C, was mainly due to the presence of amorphous carbon in the Ag incorporated activated carbon [28]. The burning of activated carbon

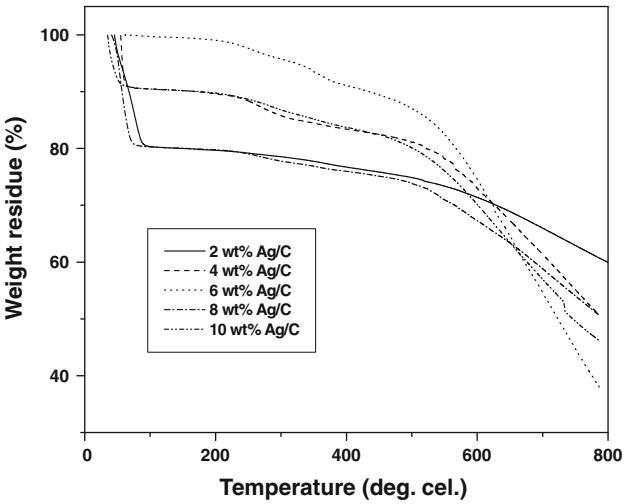

Fig. 6 Thermogravimetric curves of as-synthesized Ag/C catalysts

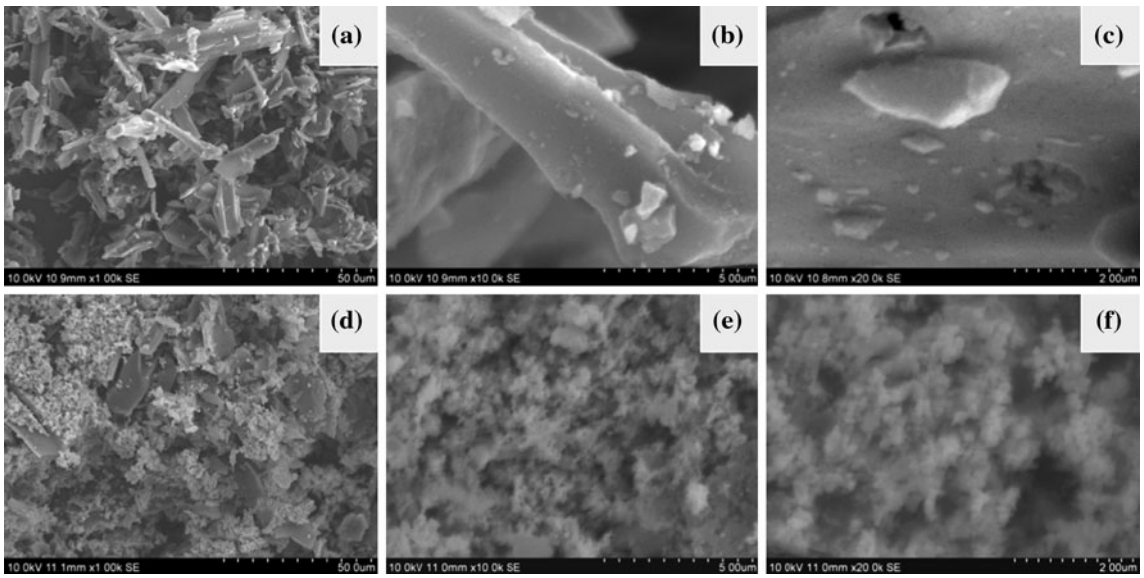

Fig. 5 SEM images of 2 wt% (**a–c**) and 10 wt% (**d–f**) carbon supported silver catalysts with different magnifications

themselves begins at around 620 °C. It was noted that approximately 40% of the sample remained after performing TGA up to 800 °C. This residue remains mainly due to the presence of Ag particles. There was no weight gain observed during thermal treatment, since no oxidation of the metal particles was expected to take place [29]. It should be noted that the prepared Ag/C catalysts can be used successfully for high temperature fuel cell application also.

Fuel cell performance study

The polarization and power density curves of 10 wt% sample, obtained from the alkaline membrane fuel cell using Pt as the anode and Ag as cathode catalyst are presented in Fig. 7. The measurements were made by feeding hydrogen and oxygen as a fuel and oxidant, respectively, at 60 °C. At low currents the region of activation polarization loss can be distinguished on the cell voltage curve, related to slow kinetics of the oxygen reduction reaction. At intermediate currents a region of ohmic polarization loss is observed and finally, at higher currents the concentration polarization loss leads to a gradual decrease of the cell voltage. The alkaline membrane fuel cell with 10 wt% Ag/C showed a maximum cell voltage of 0.69 V and power density of 109 mW/cm^2 at 60 °C.

Methanol oxidation

The dispersion of silver nanoparticles on the activated carbon support greatly affects the activity of the catalyst. Hence, the modification of the support surface to create surface functional groups compatible to Ag becomes the only choice [30]. To test the electrocatalytic behavior of Ag/C in Direct methanol alkaline fuel cell (DMAFC),

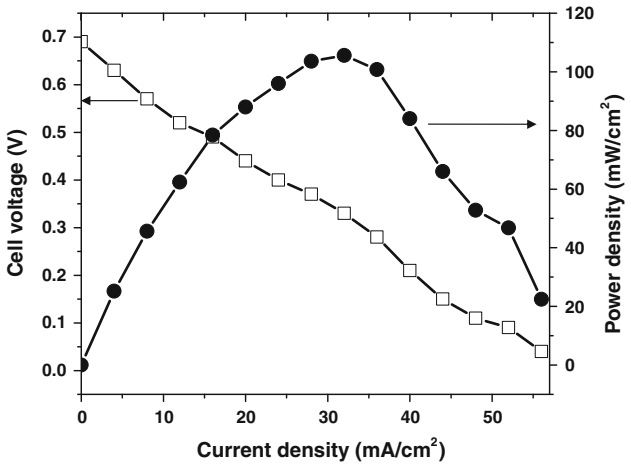

Fig. 7 Alkaline membrane fuel cell performance of QPSEBS ionomer using Pt/C as the anode and 10 wt% Ag/C as the cathode

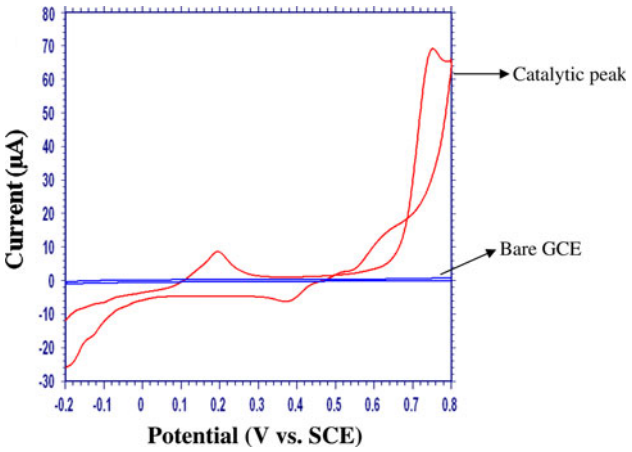

Fig. 8 Cyclic Voltammogram of Bare GCE and 10 wt% Ag/C/GCE in 1 M KOH and 1 M methanol solution

cyclic voltammograms at the bare GCE and Ag/C/GCE were recorded in the presence of 1 M KOH and 1 M methanol with potential range from −0.2 to 0.8 V (Vs. SCE) at a scan rate of 50 mVs^{-1} and the results are presented in Fig. 8. As shown in Fig. 8, at bare GCE no electrooxidation occurs. However, the electrocatalytic oxidation of methanol at the Ag/C/GC electrode can be seen clearly in the figure. Adding Ag/C catalyst on to the electrode surface, a dramatic change is observed in the CVs. A large anodic peak is observed at 0.65 V and a small peak is observed at 0.2 V. The reason is that an ideal nanoconstruction of the catalyst in the electrodes enhances their electrocatalytic activity. The peak at 0.65 V is attributed to the oxidation potential where methanol is oxidized, as reported by others. The increment of catalytic current and the decrease of overpotential which are two important factors in evaluating the catalytic effect, conclude that the as synthesized Ag/C catalyst can be effectively used in DMAFC applications.

Conclusions

We have successfully synthesized Ag incorporated carbon (Ag/C) catalyst by wet impregnation method by varying the Ag percentage. The XRD analysis revealed that the identified planes of the synthesized compound coincided well with those characteristic of Ag as per the JCPDS data and the size of the prepared Ag particles were in nanometer range, varying from 5 to 11 nm. From thermogravimetric analysis, the prepared catalysts were stable even at 800 °C indicating that it was suitable for high temperature fuel cell applications too. The degree of the graphitization of the prepared Ag/C catalyst was quantified by Raman spectroscopy. SEM analysis showed that the Ag particles were widely distributed showing some signs of agglomeration at

certain places. The surface plasma resonance bands were identified in the prepared catalysts using DRS-UV. The 10 wt% metal loaded catalysts taken for alkaline membrane fuel cell performance study, showed a maximum cell voltage of 0.69 V and power density of 109 mW/cm^2 at 60 °C. In addition, the same catalyst was subjected to electrocatalytic oxidation and the results obtained were promising.

Acknowledgement Financial support from the Department of Science and Technology (DST), New Delhi, India (Letter No. SR/S2/CMP-06/2008, dated 21-08-2008) is gratefully acknowledged.

References

1. Sammes N (2006) Fuel cell technology: reaching towards commercialization. Springer, London
2. Blomen LJMJ, Mugerwa MN (1993) Fuel cell systems. Plenum Press, New York
3. Mench MM (2008) Fuel cell engines. John Wiley and Sons Ltd., London
4. Hermanna A, Chaudhuria T, Spagnol P (2005) Int J Hydrogen Energy 30:1297
5. Steele BCH, Heinzel A (2001) Nature 414:345
6. Borup R, Meyers J (2007) Chem Rev 107:3904
7. Jacobson MZ, Colella WG, Golden DM (2005) Science 308:1901
8. Fan YZ, Hu HQ, Liu H (2007) J Power Sour 171:348
9. Matsuoka K, Chiba S, Iriyama Y, Abe T, Matsuoka M, Kikuchi K (2008) Thin Solid Films 516:3309
10. Harper GDJ (2008) Fuel cell projects for the evil genius. McGraw-Hill/TAB Electronics, London
11. Srinivasan S (2006) Fuel cells: from fundamentals to applications. Springer, New York
12. Vinodh R, Ilakkiya A, Elamathi S, Sangeetha D (2010) J Material Sci Eng B 167:43
13. Chen L, Ma D, Li X, Bao X (2006) Catal Lett 111:133
14. Auer E, Freund A, Pietsch J, Tacke T (1998) Appl Catal A 173:259
15. Mestl G, Maksimova NI, Keller N, Roddatis VV, SchlÄogl R (2001) Angew Chem Int Ed 40:2066
16. Serp P, Corrias M, Kalck P (2003) Appl Catal A 253:337
17. Siva Kumar V, Nagaraja BM, Shashikala V, Padmasri AH, Madhavendra SS, Raju BD, Rama Rao KS (2004) J Mol Catal A Chem 223:313
18. Xu JB, Zhao TS, Liang ZX (2008) J Phys Chem C 112:17362
19. Vinodh R, Padmavathi R, Sangeetha D (2011) Desalination 267:267
20. Vinodh R, Purushothaman M, Sangeetha D (2011) Int J Hydrogen Energy 36:7291
21. Han JJ, Li N, Liu DL (2009) Mater Chem Phys 115:685
22. Ershov BG, Janata E, Henglein A (1993) J Phys Chem 97:339
23. Sato K, Yoshinari T, Kintaichi Y, Haneda M, Hamada H (2003) Appl Catal B 44:67
24. Miao SJ, Wang Y, Ma D, Zhu QJ, Zhou ST, Su LL, Tan DL, Bao XH (2004) J Phys Chem B 108:17866
25. Yao N, Lordi V, Ma SX, Dujardin E, Krishnan A, Treacy MM, Ebbesen TW (1998) J Mater Res 13:2432
26. Wang S, Wang X, Jiang SP (2008) Langmuir 24:10505
27. Zhao Y, Yang X, Tian J (2009) Electrochim Acta 54:7114
28. Chen CM, Chen M, Leu FC, Hsu SY, Wang SC, Shi SC, C. F. Chen CF (2004) 13:1182
29. Hou P, Liu C, Tong Y, Xu S, Liu M, Cheng H (2001) J Mater Res 16:2526
30. Maiyalagan T (2008) Appl Catal B Env 80:286